

Supporting Information for “Image-Guided Modeling of Virus Growth and Spread”

Eric L. Haseltine, Vy Lam, John Yin, and James B. Rawlings *

Department of Chemical and Biological Engineering, University of Wisconsin-Madison

1415 Engineering Drive, Madison, WI 53706-1607, USA

December 31, 2007

*Corresponding author. E-mail: jbraw@bevo.che.wisc.edu. Fax: (608) 265-8794.

List of Figures

S1	Experimental images obtained from the dynamic propagation of VSV on BHK cells.	3
S2	Radial infection profiles obtained by averaging the experimental images of the dynamic propagation of VSV on BHK cells.	4
S3	Comparison of the experimental and predicted radial infection profiles for the dynamic propagation of VSV on BHK cells.	5
S4	Experimental images obtained from the dynamic propagation of VSV on DBT cells.	6
S5	Radial infection profiles obtained by averaging the experimental images of the dynamic propagation of VSV on DBT cells.	7
S6	Comparison of the experimental and predicted radial infection profiles for the dynamic propagation of VSV on DBT cells.	8
S7	Comparison of the experimental and predicted radial infection profiles for the dynamic propagation of VSV on DBT cells in the presence of interferon inhibitors. . .	9
S8	Profile of the initial virus concentration for the models.	10

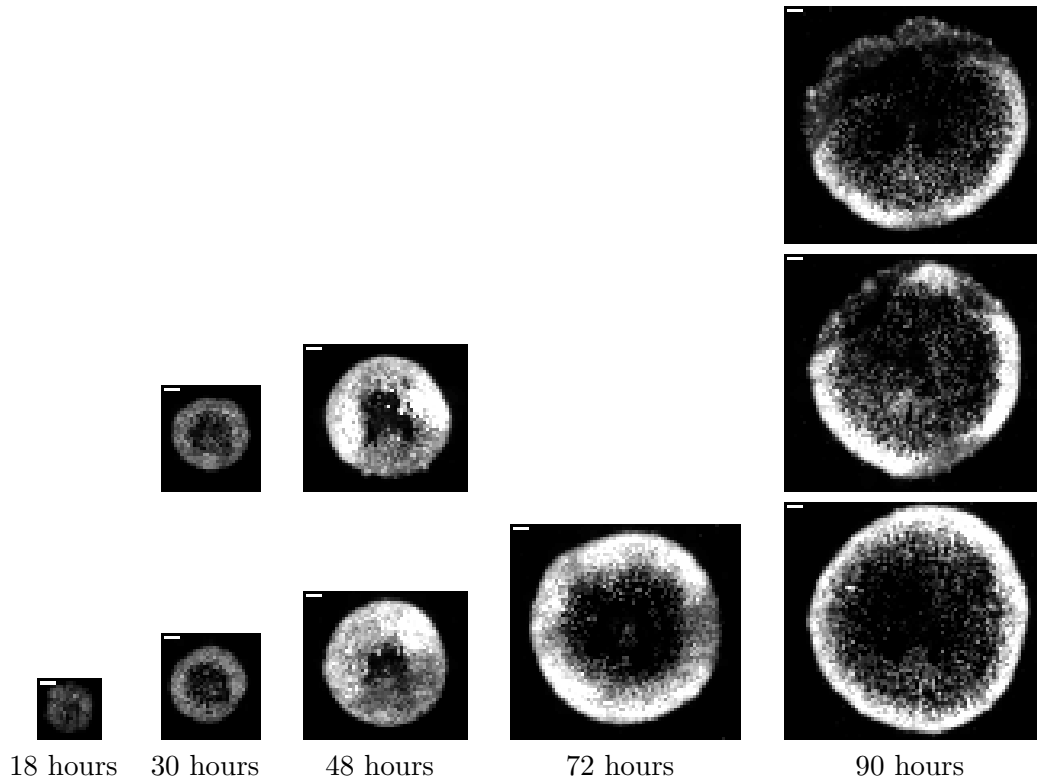


Figure S1: Experimental images obtained from the dynamic propagation of VSV on BHK cells. The white scale bar in the upper left-hand corner of the experimental images is one millimeter.

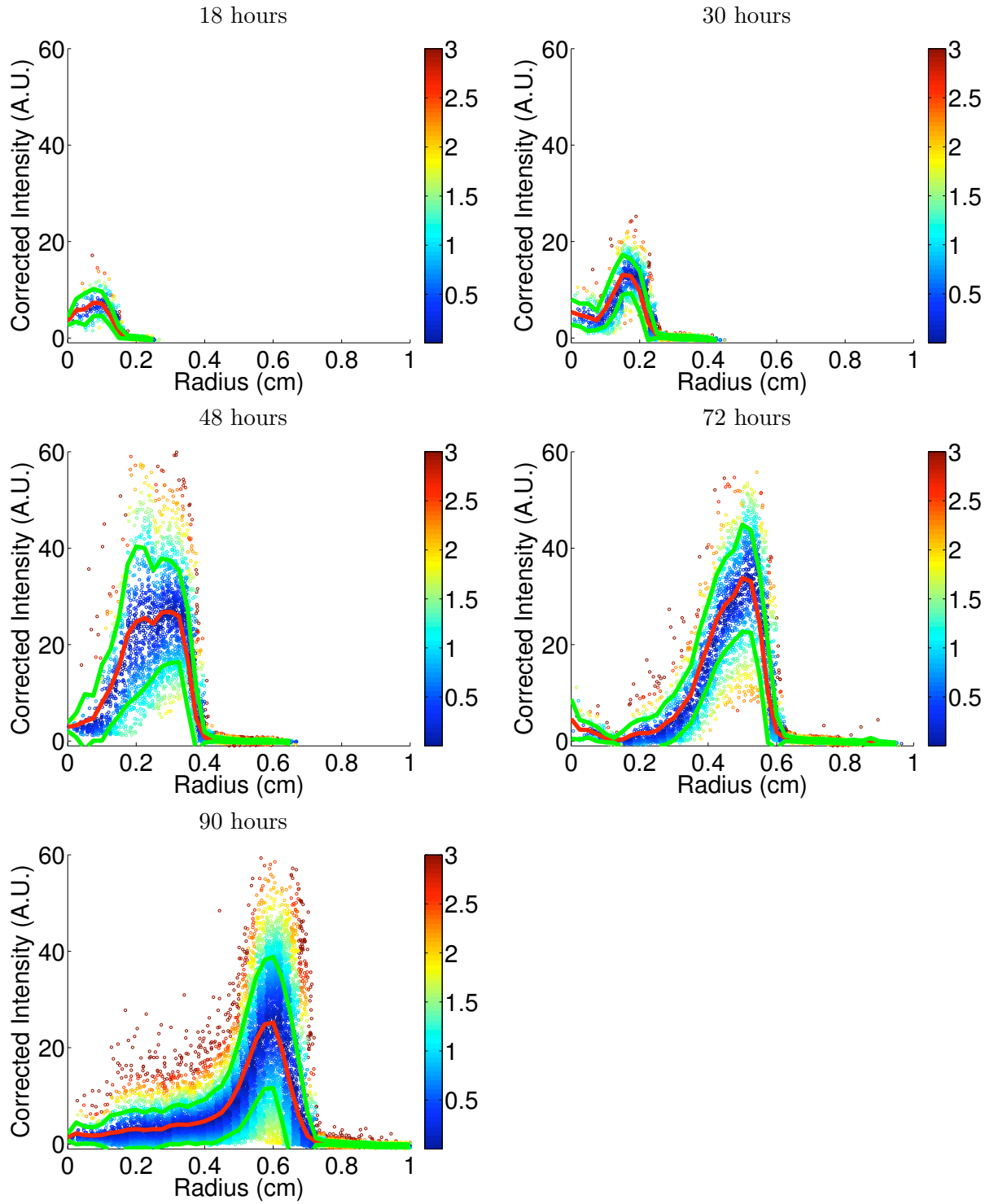


Figure S2: Radial infection profiles obtained by averaging the experimental images of the dynamic propagation of VSV on BHK cells. The color bar shows the standard deviation σ of each individual measurement from the mean value, and is saturated after $\sigma > 3$. Red lines show the average profile, and green lines show one standard deviation away from the mean. Note that the background fluorescence was estimated and subtracted from each image before calculating these radial profiles.

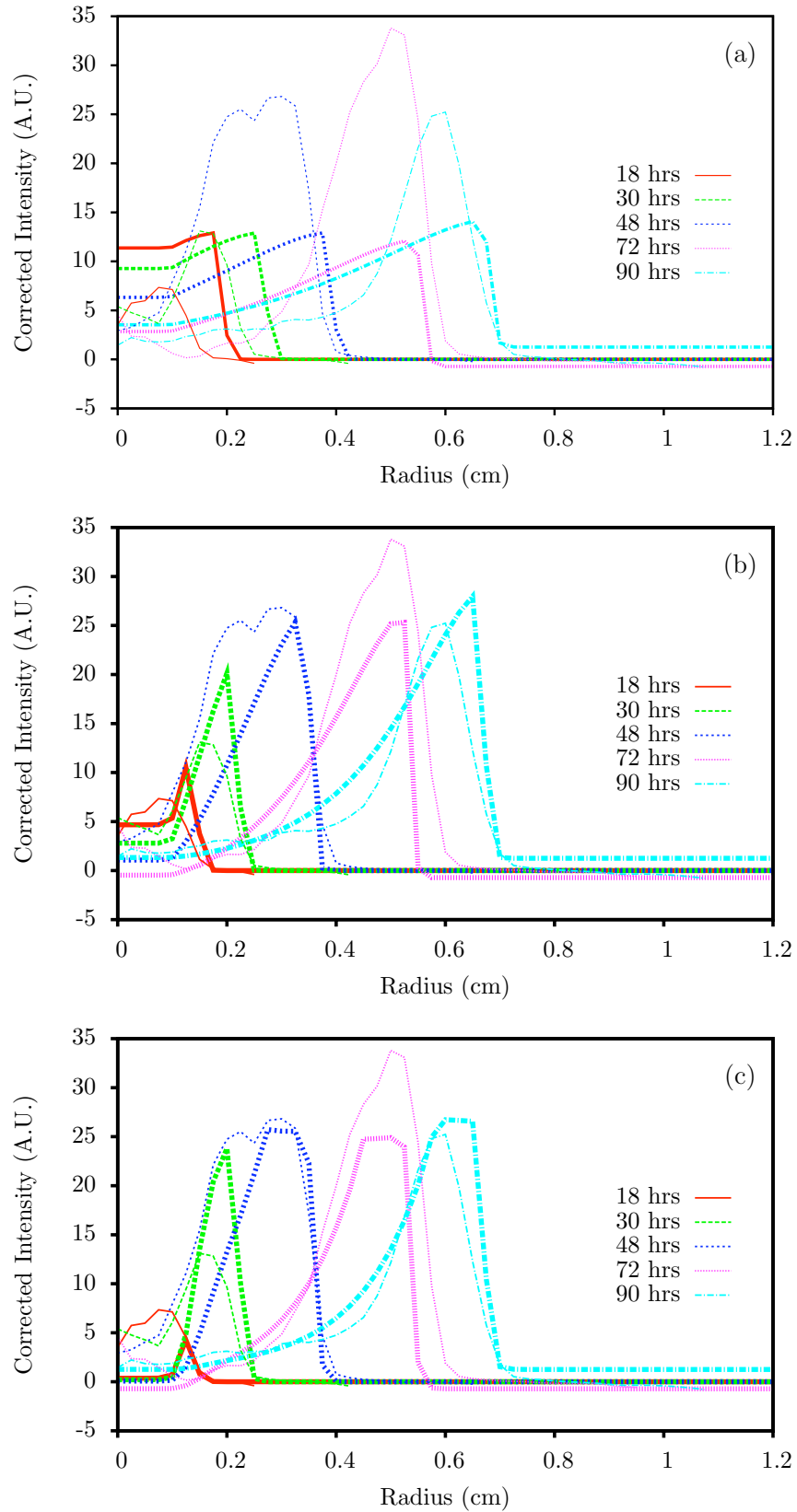


Figure S3: Comparison of the experimental and predicted radial infection profiles for the dynamic propagation of VSV on BHK cells: (a) extracellular model, no growth of uninfected cells; (b) extracellular model; and (c) age-segregated model. The thick and thin lines present the model predictions and the average experimental measurements, respectively.

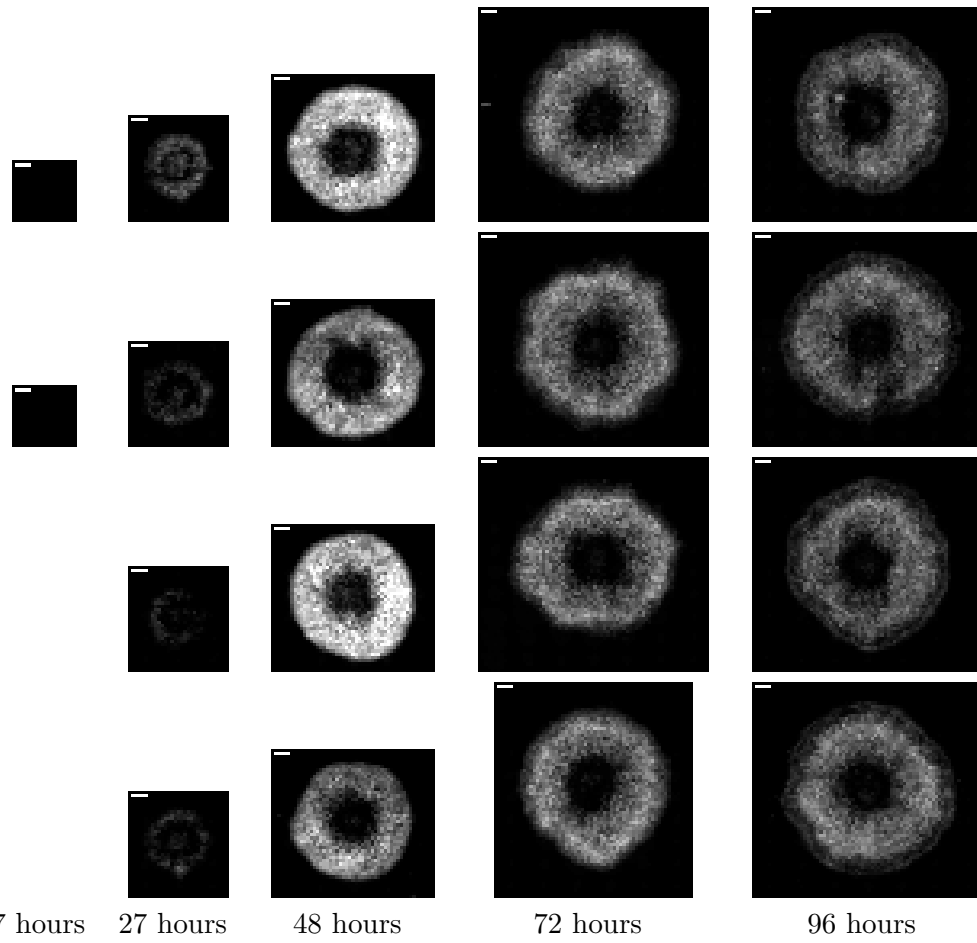


Figure S4: Experimental images obtained from the dynamic propagation of VSV on DBT cells. The white scale bar in the upper left-hand corner of the experimental images is one millimeter.

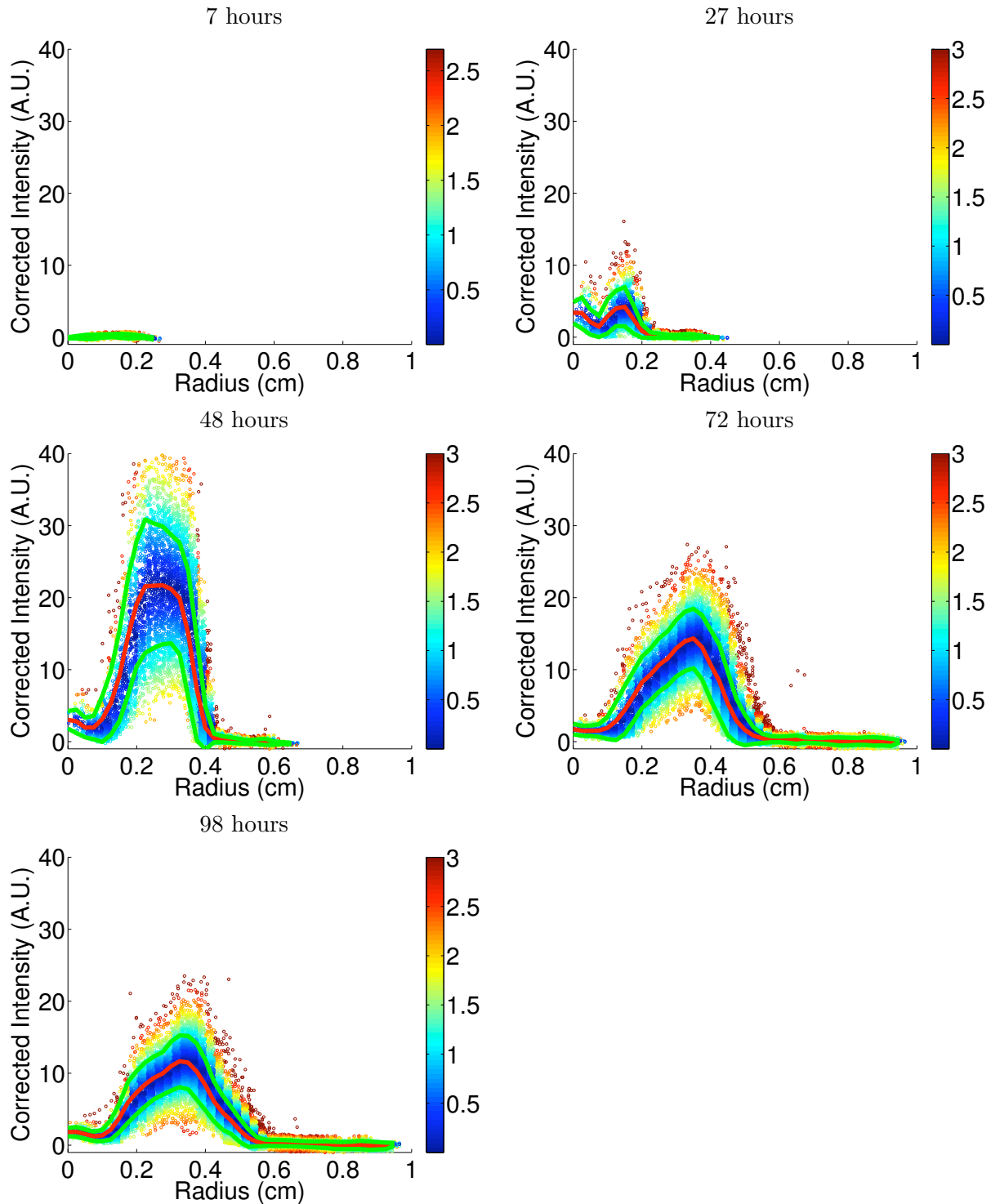


Figure S5: Radial infection profiles obtained by averaging the experimental images of the dynamic propagation of VSV on DBT cells. The color bar shows the standard deviation σ of each individual measurement from the mean value, and is saturated after $\sigma > 3$. Red lines show the average profile, and green lines show one standard deviation away from the mean. Note that the background fluorescence was estimated and subtracted from each image before calculating these radial profiles.

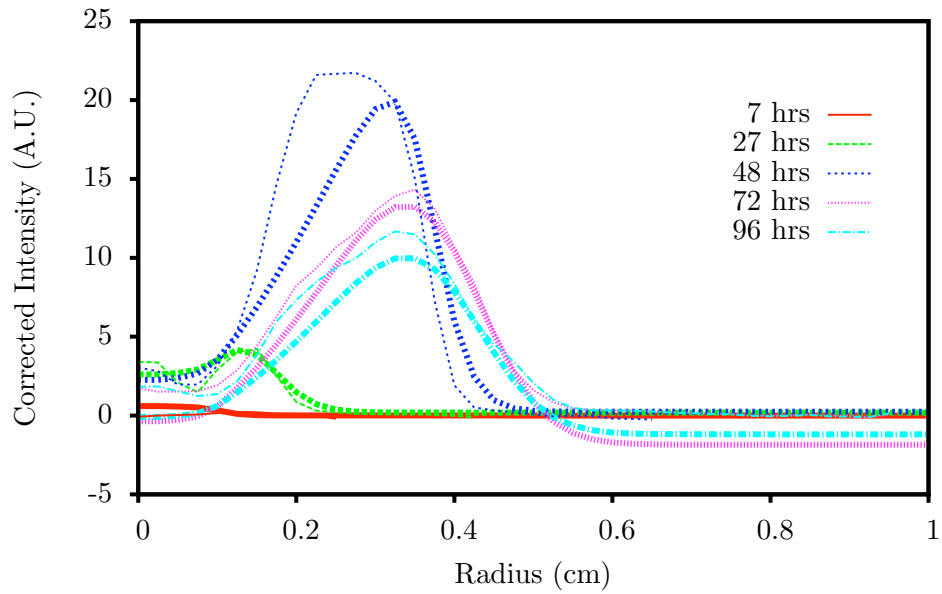


Figure S6: Comparison of the experimental and predicted radial infection profiles for the dynamic propagation of VSV on DBT cells. A reaction-diffusion model accounting for solely extracellular species generated the predicted profiles. The thick and thin lines present the model predictions and the average experimental measurements, respectively.

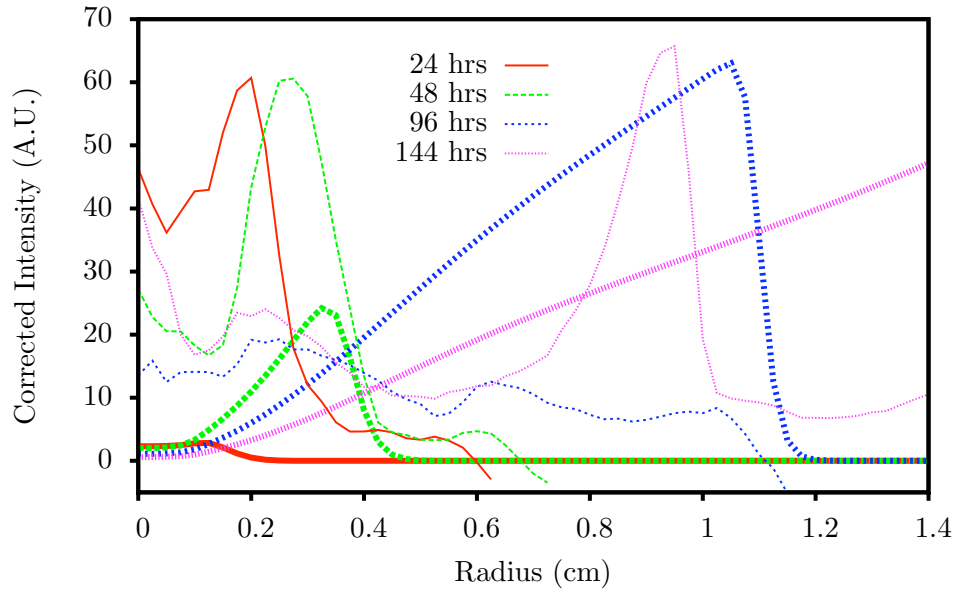


Figure S7: Comparison of the experimental and predicted radial infection profiles for the dynamic propagation of VSV on DBT cells in the presence of interferon inhibitors. A reaction-diffusion model accounting for solely extracellular species generated the predicted profiles. The thick and thin lines present the model predictions and the average experimental measurements, respectively.

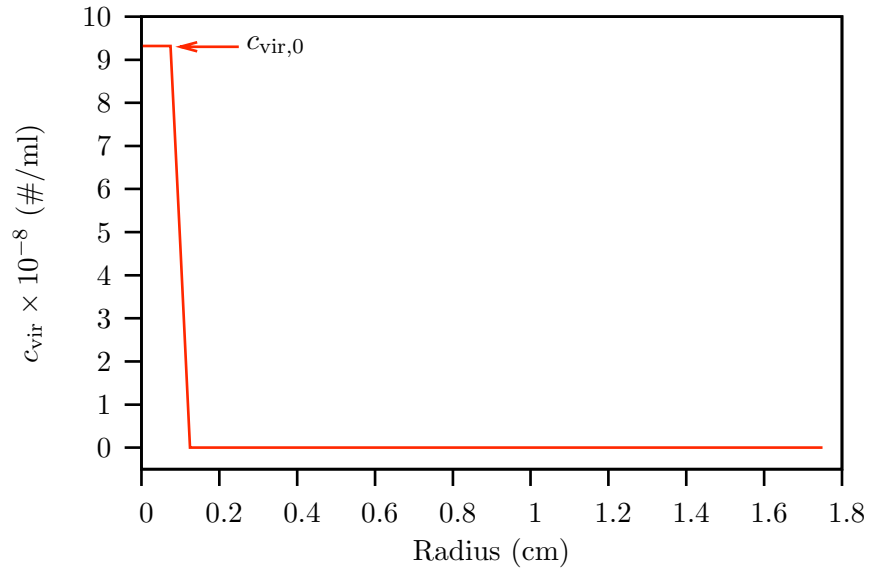


Figure S8: Profile of the initial virus concentration for the models. $c_{\text{vir},0}$ denotes the estimated initial concentration of virus in the inoculation radius.